Biogas production from grape pomace: Thermodynamic model of the process and dynamic model of the power generation system☆

C.X. Cáceres [a,*], R.E. Cáceres [a], D. Hein [b,**], M.G. Molina [c], J.M. Pia [a]

[a] Department of Chemical Engineering, Faculty of Engineering, Universidad Nacional de San Juan, Av. Libertador San Martín Oeste, 1109, J5400ARL San Juan, Argentina
[b] Department of Energy and Environmental Process Engineering, Department of Mechanical Engineering, Universität Siegen, Siegen, Germany
[c] Instituto de Energía Eléctrica, Universidad Nacional de San Juan, Av. Libertador San Martín Oeste, 1109, J5400ARL San Juan, Argentina

ABSTRACT

In year 2010, the Province of San Juan — Argentina (South America) produced around 81 947 tons of grape pomace, which is a winery waste by-product. Wineries demand a great quantity of power during the three months that winemaking time lasts, which involve a high installed electric power. This power is used mainly for refrigerating the must during the fermentation. The control of temperature is crucial in winemaking as the low temperature preserves subtle fruit characters. An alternative for reducing the requirement of power from the utility electric grid is producing it locally, using the residuals generated by the own wineries. The technology for bioenergy conversion proposed to be implemented in this research for electricity generation is the anaerobic digestion of grape pomace. The aim of this research is to develop the thermodynamic equilibrium analysis of grape pomace anaerobic digestion based on the equilibrium constants for predicting the potential production of biogas and its composition. In addition, a dynamic model of a biogas-fuelled microturbine system for distributed generation applications is derived.
Copyright © 2012, Hydrogen Energy Publications, LLC. Published by Elsevier Ltd. All rights reserved.

1. Introduction

The main environmental impacts produced by wineries activities correspond to pomace generation (residuals solid) and wastewater coming from the wash of equipment and fermentation tanks. The grape pomace and the wastewater possess very high levels of biochemical oxygen demand (BOD) and chemical oxygen demand (COD); for that, if it is not treated, they can be easily attacked by microorganisms generating foul odour and contamination problems inside the winery.

In wineries of the Province of San Juan — Argentina (South America) the wastewater is generally treated; although, the grape pomace is sold to the companies that produce ethylic alcohol, tartaric acid and grape seeds oil. The trade of the grape pomace is very low (US$ 5 per ton); however when the grape pomace is removed, the winery is left clean and tidy. The compost production from the solid residues (aerobic

fermentation) is carried out in only 5% of the wineries of San Juan.

It is estimated that in 2010, San Juan produced about 81 947 tons of grape pomace [1], considering that grape pomace represents 12%−14% of fresh grape weight [2] and the grape production for making wines and musts rises to 11 472 tons.

Wineries demand a great quantity of energy during the three months that winemaking time lasts, which involves a high installed power capacity. This energy is used mainly for refrigerating the must in fermentation, which reaches approximately to 35.39 kcal per litre of must, since grapes in San Juan arrive wineries with an average of 26° Brix. This represent a high amount of energy, considering that the volume of fermentation tanks is usually of 30 000 L and must temperature should not exceed 15 °C in white wines and 26 °C in red ones. The control of temperature is crucial in wine-making provided that the cooling temperature preserves subtle fruit characters.

In Argentina, the cost of the electric power is compound of both a fixed component and a variable one. The fixed component is a function of the installed power. The variable component is proportional to the amount of energy consumed in the billing period.

Due to the high installed power capacity, during the nine months that wineries are not active the energy costs stay high. A form of diminishing the requirement of energy from the electric system is by producing it locally, using the residuals generated by the own wineries. This generation type is denominated in situ or distributed generation (DG), and constitutes a radical change of the paradigm of the conventional electric power generation.

In the last years, the use of various kinds of biomass for producing heat and electricity has been increased [3]. The main advantage for that are the reduction of greenhouse gas (GHG) and other pollutant emissions [2].

The technology for bioenergy conversion proposed to be implemented in this research for electricity production is the anaerobic digestion of grape pomace. The selection of this technology has been carried out keeping in mind the following considerations:

- Characteristic of the waste use: grape pomace is a high strength organic waste with low levels of nitrogen and phosphorous with sufficient trace elements for bacterial growth [4]. In addition, the humidity of the grape pomace, which varies between 25% and 65% [5] is not a problem for anaerobic digestion, however, restrict the implementation of others technologies for conversion of biomass.
- Characteristics of the processes for biogas production: from anaerobic digestion, biogas is obtained at atmospheric pressure and lower temperatures than the gases obtained with other technologies for conversion of biomass, so that plants are comparatively easier to operate and costs of initial investment are lower [6] than that for other technologies.

The aim of this work is to develop the thermodynamic equilibrium model of grape pomace anaerobic digestion based on equilibrium constant in order to determine the optimum operating conditions and subsequently predicting the

composition of the produced biogas. With these results, a dynamic model of a biogas-fuelled microturbine system for distributed generation applications is derived. In this way, the global system enables to generate power from the solid waste of the own wineries (grape pomace); thus reducing the power requirements of a winery, especially during its larger demand periods.

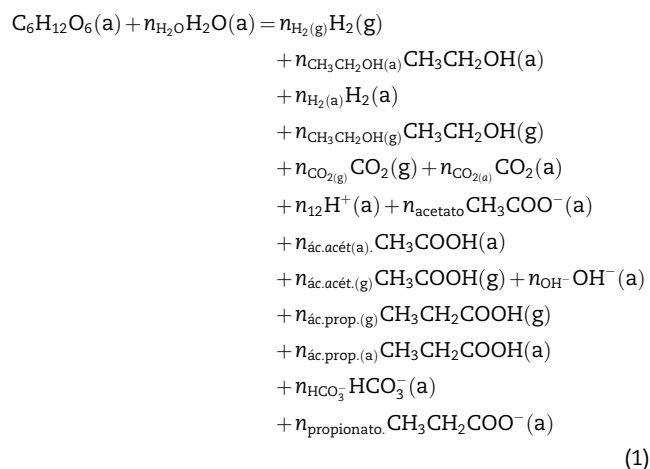## 2. Thermodynamic model of the biogas production process

For the development of the model it was considered that the anaerobic digestion process could be divided into three phases, i.e. hydrolysis, acid formation and methane formation.

2.1. Phase of hydrolysis

In this first phase, the complex structure of organic matter is broken down into its fundamental parts during the hydrolysis process: the proteins are converted into amino acids, complex carbohydrates such as cellulose, lignin, starch and fibres are transformed into simple sugars, like glucose [7]. This phase is not considered for the development of this model.

2.2. Phase of acids formation

This phase includes acidogenesis and acetogenesis, and can be expressed by the following general reaction:

$$
\begin{aligned}
C_6H_{12}O_6(a) + n_{H_2O}H_2O(a) = {} & n_{H_2(g)}H_2(g) \\
& + n_{CH_3CH_2OH(a)}CH_3CH_2OH(a) \\
& + n_{H_2(a)}H_2(a) \\
& + n_{CH_3CH_2OH(g)}CH_3CH_2OH(g) \\
& + n_{CO_2(g)}CO_2(g) + n_{CO_2(a)}CO_2(a) \\
& + n_{12}H^+(a) + n_{acetato}CH_3COO^-(a) \\
& + n_{ác.acét(a).}CH_3COOH(a) \\
& + n_{ác.acét.(g)}CH_3COOH(g) + n_{OH^-}OH^-(a) \\
& + n_{ác.prop.(g)}CH_3CH_2COOH(g) \\
& + n_{ác.prop.(a)}CH_3CH_2COOH(a) \\
& + n_{HCO_3^-}HCO_3^-(a) \\
& + n_{propionato.}CH_3CH_2COO^-(a)
\end{aligned}
$$

(1)

being n_i the number of moles of species i; which are unknown.

In order to determine the n_i values, a system of equations is proposed, which include the mass balance equations and the equilibrium constants equations of reactions occurring in this stage. In this way, the mass balance equation for carbon is defined by Eq. (2). Analogously, the mass balance equations for oxygen and hydrogen are determined.
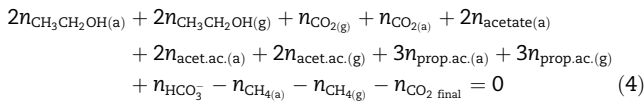
$$
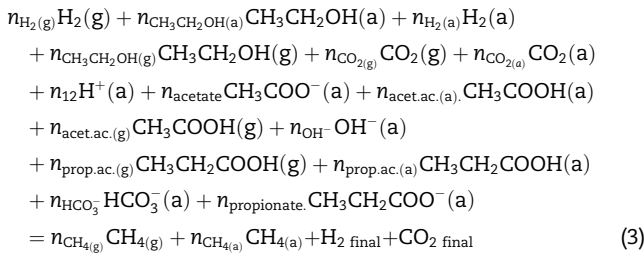\begin{aligned}
2n_{CH_3CH_2OH(a)} + 2n_{CH_3CH_2OH(g)} + n_{CO_2(g)} + n_{CO_2(a)} + 2n_{acetato(a)} \\
+ 2n_{ác.acét.(a)} + 2n_{ác.acét.(g)} + 3n_{ác.prop.(a)} + 3n_{ác.prop.(g)} \\
+ n_{HCO_3^-} + 3n_{propionato(a)} - 6 = 0
\end{aligned}
$$

(2)

The redox equilibrium, electrochemical equilibrium and phase equilibrium reactions in the phase of acid formation are

shown in Table 1 [7]. These equations are used as a basis in order to get the equilibrium constants equations of this stage.

2.3. Phase of methane formation

The phase of methane formation can be described by Eq. (3). In order to determine the n_i values, a system of equations is proposed, which include the mass balance equations and the equilibrium constants equations of reactions occurring in this stage. In this way, the mass balance equation for carbon is defined by Eq. (4). In the same way, the mass balance equations for oxygen and hydrogen are derived.

$$n_{\text{H}_2(\text{g})}\text{H}_2(\text{g}) + n_{\text{CH}_3\text{CH}_2\text{OH}(\text{a})}\text{CH}_3\text{CH}_2\text{OH}(\text{a}) + n_{\text{H}_2(\text{a})}\text{H}_2(\text{a})$$
$$+ n_{\text{CH}_3\text{CH}_2\text{OH}(\text{g})}\text{CH}_3\text{CH}_2\text{OH}(\text{g}) + n_{\text{CO}_2(\text{g})}\text{CO}_2(\text{g}) + n_{\text{CO}_2(\text{a})}\text{CO}_2(\text{a})$$
$$+ n_{12}\text{H}^+(\text{a}) + n_{\text{acetate}}\text{CH}_3\text{COO}^-(\text{a}) + n_{\text{acet.ac.(a)}}\text{CH}_3\text{COOH}(\text{a})$$
$$+ n_{\text{acet.ac.(g)}}\text{CH}_3\text{COOH}(\text{g}) + n_{\text{OH}^-}\text{OH}^-(\text{a})$$
$$+ n_{\text{prop.ac.(g)}}\text{CH}_3\text{CH}_2\text{COOH}(\text{g}) + n_{\text{prop.ac.(a)}}\text{CH}_3\text{CH}_2\text{COOH}(\text{a})$$
$$+ n_{\text{HCO}_3^-}\text{HCO}_3^-(\text{a}) + n_{\text{propionate}}\text{CH}_3\text{CH}_2\text{COO}^-(\text{a})$$
$$= n_{\text{CH}_4(\text{g})}\text{CH}_4(\text{g}) + n_{\text{CH}_4(\text{a})}\text{CH}_4(\text{a}) + \text{H}_2\text{ final} + \text{CO}_2\text{ final} \quad (3)$$

$$2n_{\text{CH}_3\text{CH}_2\text{OH}(\text{a})} + 2n_{\text{CH}_3\text{CH}_2\text{OH}(\text{g})} + n_{\text{CO}_2(\text{g})} + n_{\text{CO}_2(\text{a})} + 2n_{\text{acetate(a)}}$$
$$+ 2n_{\text{acet.ac.(a)}} + 2n_{\text{acet.ac.(g)}} + 3n_{\text{prop.ac.(a)}} + 3n_{\text{prop.ac.(g)}}$$
$$+ n_{\text{HCO}_3^-} - n_{\text{CH}_4(\text{a})} - n_{\text{CH}_4(\text{g})} - n_{\text{CO}_2\text{ final}} = 0 \quad (4)$$

The redox equilibrium, electrochemical equilibrium and phase equilibrium reactions in the phase of methane formation are shown in Table 2 [7]. These equations are used as a basis in order to get the equilibrium constants equations of this stage.

The proposed thermodynamic model is developed on the basis of the equilibrium constants. These constants, in the case of liquids, are expressed in terms of activity (a_i):

$$K = \prod_i (a_i)^{\nu_i} \quad (5)$$

where ν_i are the stoichiometrics coefficients, which have positive values for the products and negatives values for the reactants. The activity can be written as a function of the activity coefficient (γ_i) and molar fraction in liquid (x_i):

$$a_i = \gamma_i x_i \quad (6)$$

By replacing Eq. (6) in Eq. (5) and considering that solutions are ideal ($\gamma_i = 1$) for the developed model, then the constant K is:

$$K = \prod_i (x_i)^{\nu_i} \quad (7)$$

In the case of gases, the equilibrium constants can be expressed as a function of fugacity (f_i), as follows:

$$K = \prod_i (f_i)^{\nu_i} \quad (8)$$

The fugacity is stated as a function of the fugacity coefficient (ϕ), the molar fraction in the gas (y_i) and the total pressure (P), in the following way:

$$f_i = \phi_i y_i p \quad (9)$$

By replacing Eq. (9) in Eq. (8) and considering that $P=1$ and the gases of the system are ideal ($\phi = 1$) for the proposed model, then K can be expressed as:

$$K = \prod_i (y_i)^{\nu_i} \quad (10)$$

2.4. Solution of the system of equations of the proposed thermodynamic model

The system of equations proposed to describe the acid formation phase is composed of the mass balance equations for carbon, oxygen and hydrogen and the equilibrium constants equations of reactions occurring in this stage, which are exposed in Table 1 according to Eq. (7). Analogously, the system of equations proposed to describe the acid formation phase is constituted by the mass balance equations for carbon, oxygen and hydrogen and the equilibrium constants equations of reactions occurring in this other stage, which are exposed in Table 2 according to Eq. (8). The values of

Table 1 – Stoichiometric equations evolved in the acids formation phase during the anaerobic digestion.		
Redox equilibrium	Electrochemical equilibrium	Phase equilibrium
$\text{C}_6\text{H}_{12}\text{O}_6(\text{a}) + 2\text{H}_2\text{O} = 2\text{CH}_3\text{COOH}(\text{a})$ $+ 2\text{CO}_2(\text{a}) + 4\text{H}_2(\text{a})$	$\text{CH}_3\text{CH}_2\text{COO}^-(\text{a}) + 3\text{H}_2\text{O}(\text{a}) = \text{H}^+(\text{a}) + \text{CH}_3\text{COO}^-(\text{a})$ $+ \text{HCO}_3(\text{a}) + 3\text{H}_2(\text{a})$	$\text{CH}_3\text{CH}_2\text{COOH}(\text{a}) = \text{CH}_3\text{CH}_2\text{COOH}(\text{g})$
$\text{C}_6\text{H}_{12}\text{O}_6(\text{a}) + 2\text{H}_2(\text{g}) = 2\text{H}_2\text{O}(\text{a})$ $+ 2\text{CH}_3\text{CH}_2\text{COOH}(\text{a})$	$\text{CH}_3\text{CH}_2\text{COH}(\text{g}) + 3\text{H}_2\text{O}(\text{a}) = \text{CH}_3\text{COO}^-(\text{a}) + 2\text{H}_2(\text{a}) + \text{H}^+(\text{a})$	$\text{CH}_3\text{COOH}(\text{a}) = \text{CH}_3\text{COOH}(\text{g})$
$\text{C}_6\text{H}_{12}\text{O}_6(\text{a}) = 2\text{CH}_3\text{CH}_2\text{OH}(\text{g})$ $+ 2\text{CO}_2(\text{g})$	$2\text{HCO}_3^-(\text{a}) + 4\text{H}_2(\text{a}) + \text{H}^+(\text{a}) = \text{CH}_3\text{COO}^-(\text{a}) + 2\text{H}_2\text{O}(\text{a})$	$\text{CH}_3\text{CH}_2\text{OH}(\text{a}) = \text{CH}_3\text{CH}_2\text{OH}(\text{g})$
	$\text{CH}_3\text{CH}_2\text{COOH}(\text{a}) = \text{CH}_3\text{CH}_2\text{COO}^-(\text{a}) + \text{H}^+(\text{a})$ $\text{CH}_3\text{COOH}(\text{a}) = \text{CH}_3\text{COO}^-(\text{a}) + \text{H}^+(\text{a})$ $\text{CO}_2(\text{a}) + \text{H}_2\text{O}(\text{a}) = \text{HCO}_3^-(\text{a}) + \text{H}^+(\text{a})$ $\text{H}_2\text{O}(\text{a}) = \text{H}^+(\text{a}) + \text{OH}^-(\text{a})$	$\text{H}_2(\text{a}) = \text{H}_2(\text{g})$ $\text{CO}_2(\text{a}) = \text{CO}_2(\text{g})$

Table 2 − Stoichiometric equations evolved in metanogenesis phase during the anaerobic digestion.

Redox equilibrium	Electrochemical equilibrium	Phase equilibrium
$2CH_3CH_2OH(g)+CO_2(a)= 2CH_3COOH(a)+CH_4(a)$	$CH_3COOH(a)= CH_3COO^-(a) + H^+(a)$	$CH_4(a)= CH_4(g)$
$CH_3COOH(a)= CH_4(a)+CO_2(a)$	$CO_2(a)+H_2O(a)= HCO_3^-(a) + H^+(a)$	$CH_3COOH(a)= CH_3COOH(g)$
$CH_3CH_2OH(g)+2H_2(a)= 2CH_4(a)+H_2O(a)$	$H_2O(a) = H^+(a) + OH^-(a)$	$CH_3CH_2OH(a)= CH_3CH_2OH(g)$
$CO_2(a)+4H_2(a)= CH_4(a)+2H_2O(a)$		$H_2(a)= H_2(g)$
		$CO_2(a)= CO_2(g)$

the equilibrium constants are extracted from literature [8−10]. The Newton−Raphson method is applied in order to solve the system of equations used to describe the acid formation phase and the methane formation phase and to determine thus the values of n_i. The convergence criteria for solution of all equations were set at 1.0×10^{-14}.

3. Dynamic model of the microturbine system

3.1. Overview of the biogas-fuelled microturbine system

Microturbines (MTs) demonstrate some unique attributes for running on biogas that enable them to compete against reciprocating engines, particularly at smaller sites. In fact, biogas applications are among the most promising recent applications for microturbines. Biogas is available from many sources of organic waste, such as landfill sites, wastewater treatment plants, agricultural and livestock operations, food processing plants, gasified woody biomass, among others. In the proposed application, biogas is produced through the anaerobic decomposition of organic materials from grape pomace, a waste of wineries.

Nowadays, MT manufacturers have modified their systems to better handle the unique qualities of this waste biogas and the impurities it contains, yielding the so-called renewable microturbines. The combustible portion of this gas is methane (CH_4), while most of the rest is CO_2, with small amounts of nitrogen, oxygen, hydrogen, water (the biggest source of problems in biogas applications), hydrogen sulphide and trace elements. So the best environmental solution is to use these waste gases to generate renewable power, and microturbines can do it efficiently, reliably, cleanly and economically.

Microturbines are small, compact, lightweight, and simple-cycle gas turbines used for stationary energy generation applications with outputs ranging from around 25−300 kW. They are a part of a general evolution in gas turbine technology. These systems are high speed turbines (50 000 to 120 000 rpm) with air foil bearings. Its thermal efficiency is more than 30%. A microturbine system, as shown in Fig. 1, is made up of a gas combustion microturbine engine directly coupled (gearless) to a multi-pole permanent magnet synchronous generator (PMSG) that produces electrical power operating at high speeds. The high-frequency electrical power (up to 1600 Hz) is converted to DC voltage and then inverted back to low frequency (50 or 60 Hz) AC voltage through an electronic power conditioning system (PCS). The PCS is basically composed of a three-phase rectifier bridge and a DC/AC voltage source inverter. The connection to the electric distribution grid is made through a step-up transformer and a low pass filter.

The model of the microturbine system presented in this work is based on the following assumptions:

- The microturbine engine is similar to a conventional gas combustion turbine, but smaller in size and spinning at higher speeds.
- The microturbine system shares a single rotating shaft including the MT engine and the generator.
- A permanent magnet synchronous generator is used to generate the three-phase AC power.
- The power conditioning system employed, which is described in-depth in [11], uses a rectifier and an inverter for connecting the microturbine to the distribution grid.

3.2. Model of the microturbine engine

Analogous to a typical combustion gas turbine, the biogas microturbine engine mainly involves an air compression section, a burner or combustion chamber for ignition of input renewable fuel, a pre-treatment system to achieve the desired biogas quality, a recuperator of thermal energy from exhaust gases for improving overall electrical efficiency, and a power microturbine driving the generator, as depicted in Fig. 2.

Based on the above considerations, the microturbine engine dynamics can by modelled as a conventional small gas turbine. The dynamic model of a combustion gas turbine is widely discussed in [12,13]. In this research, a simplified single shaft gas microturbine and all its control systems have been implemented to represent its dynamics. The control system consists mainly of a speed governor, an exhaust gases temperature control and a fuel (biogas) injection control (also known as acceleration control). These three controls are implemented in MATLAB/Simulink, as shown in Fig. 3.

The speed controller is a proportional-integral (PI) block, which includes a droop feedback in order to allow either droop
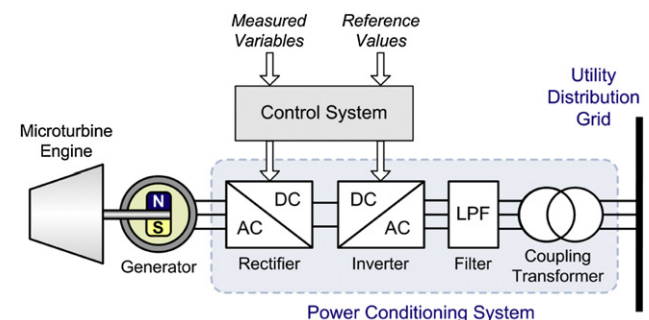

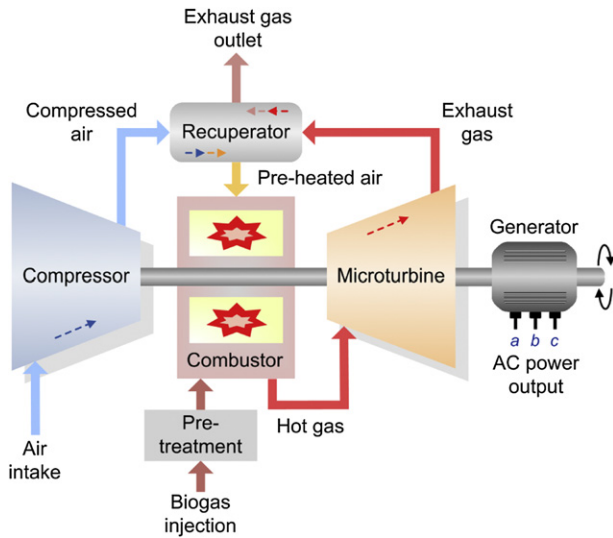Fig. 1 − Schematic diagram of the microturbine system.

Fig. 2 – Simplified scheme of a biogas microturbine engine coupled to the generator.

Fig. 4 – Variation of thermodynamic equilibrium composition with operating temperature for the produced biogas.

or isochronous operation of the microturbine system. The signal for the speed governor results from a comparison of the microturbine actual and reference (desired) speed and its limits restriction to its admissible values. The temperature control and acceleration control have no impact on the normal operating conditions. The acceleration control loop usually intervenes during start-up transients and in case of fast reductions of the system load by controlling the fuel (biogas) injection for the turbine. In these cases, the amount of injected gas (in gram per minute) is governed by a valve positioner controlled by the turbine speed controller signal (D comb). The microturbine temperature control loop implements a limit to the microturbine output power in case of a too high temperature of its exhaust gases, by acting over the gas injection flow control.

4. Simulations and results

The results from solving the system equations that describe the anaerobic digestion are shown in Fig. 4. As can be seen, the conversion of glucose is almost completely in CO_2 y CH_4,
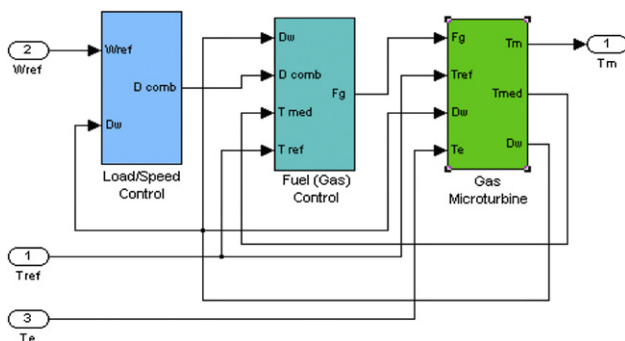

Fig. 3 – MATLAB/Simulink model of the microturbine with its main controls (acceleration, speed, and temperature control).
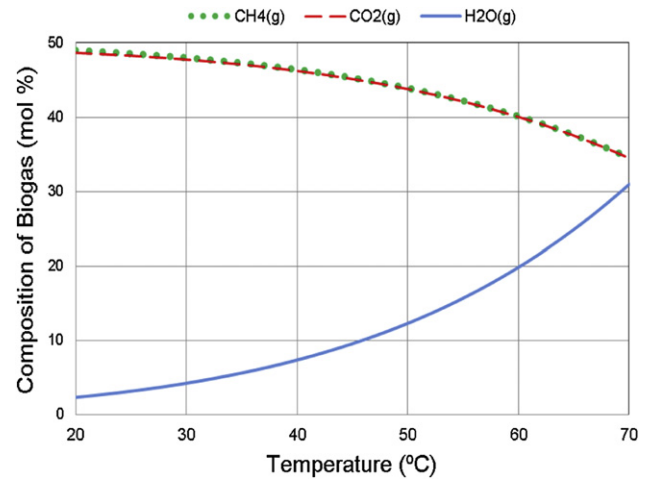
besides there being as a product a small amount of the steam. The composition of biogas produced at different operating temperatures is presented in Table 3. From the thermodynamic point-of-view, the composition of biogas at 20 °C is 49% in moles of CH_4, 48% in moles of CO_2 and 2.336% in moles of steam. While temperature varies, the fractions of CO_2 and CH_4 in the biogas are decreased. In the case of the steam, it shows a reverse trend. Fig. 5 depicts with more precision that exists a higher level of methane in the biogas composition; being this proportion a function of temperature.

Applying the results obtained from the proposed model and assuming that dry grape pomace contain 20% glucose (w/w) [14], it can be concluded that it is possible to obtain 93 784 kWh per 1000 tons of grape crush.

The dynamic performance of the proposed full modelling of the biogas-fuelled microturbine system is assessed through digital simulations carried out in MATLAB/Simulink [15], by using SimPowerSystems. To this aim, simulation has been performed in discrete time with a fixed-step size of 25 μs in order to study the response of a 20 kW MT to a variation in the power set-point. The microturbine operates connected to a low-voltage distribution grid (380 V/50 Hz), which is modelled as an infinite bus with 10 MW short circuit power

Components (% in moles)	Temperature (°C)		
	20	50	70
CH_4 (g)	49.00	43.85	34.53
CO_2 (g)	48.66	43.72	34.48
H_2O (g)	2.34	12.43	30.98
H_2 (g)	1.25×10^{-4}	1.41×10^{-3}	5.43×10^{-3}
CO (g)	1.92×10^{-8}	1.76×10^{-7}	5.17×10^{-7}
$C_2H_4O_2$ (g)	2.05×10^{-11}	5.88×10^{-11}	7.41×10^{-11}
$C_3H_6O_2$ (g)	1.35×10^{-16}	3.34×10^{-16}	4.65×10^{-16}
C_2H_6O (g)	5.55×10^{-18}	7.54×10^{-17}	2.28×10^{-16}
$C_4H_8O_2$ (g)	3.42×10^{-22}	4.98×10^{-22}	3.10×10^{-22}

Table 3 – Composition of the produced biogas at different operating temperatures.
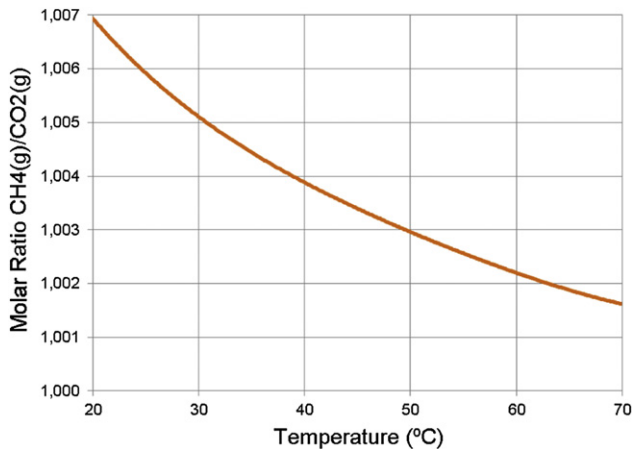
Fig. 5 – Effect of operating temperature on molar ratio CH₄ (g)/ CO₂ (g) for the produced biogas.

level and is completed with a three phase load (38 kW/ 29 kvar), representing a typical peak demand of a winery with an average production of about 1 million litres. For the electric grid simulation, the following assumptions are made: voltages and currents of the AC source are sinusoidal and symmetrical, MT generator dynamics and saturations are neglected, and loads are linear and balanced.

In the simulations shown in Fig. 6, an active power command is set to the MT set-point in order to make a step change of 20 kW at $t = 0.3$ s (red dashed lines of Fig. 3(a)). As a consequence of this step increase in the power set-point, the
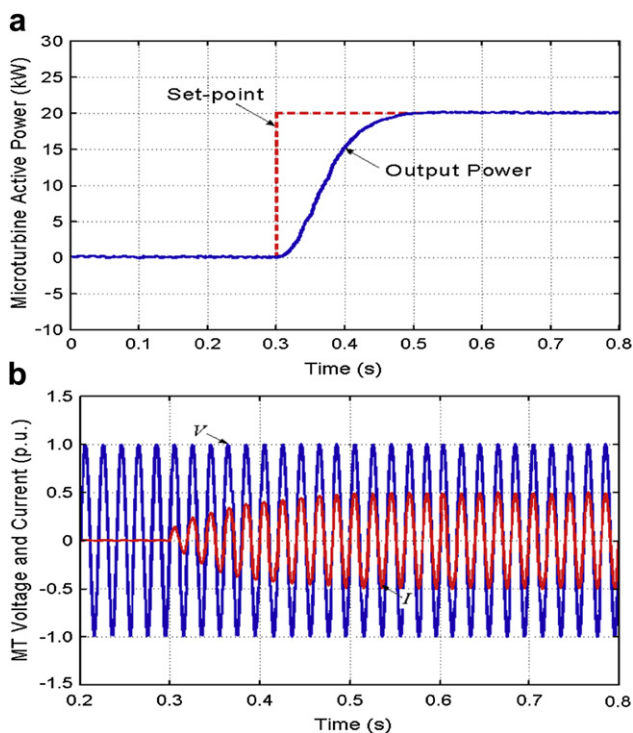
microturbine increases its active power output to deliver its full power in the way shown in Fig. 6(a) with blue solid lines. Under these circumstances, Fig. 6(b) shows the microturbine phasé á voltage at its output terminals (blue solid lines) in p.u. of 220 V, which is in-phase with the output current (red solid lines) during the active power injection.

5. Conclusion

In this paper, the development of a thermodynamic model of anaerobic digestion for predicting the potential production of biogas and its composition has been presented. In addition, a dynamic model of a biogas-fuelled microturbine system for distributed generation applications has been developed using the MATLAB/Simulink software. This model can be exploited in dynamic studies for the evaluation of the effects of incorporating microturbines powered by various renewable fuels in distribution networks. Simulation results permit to conclude that the biogas-fuelled microturbine works properly connected to a low-voltage distribution grid, enabling to reduce the power requirements of a winery, especially during its larger demand periods, by using the waste generated by the own wineries. The results obtained have shown that it is possible to obtain 93 784 kWh per 1000 tons of grape crushed. Considering that the biogas microturbine electric efficiency is on average 33%, approximately 30 948 kWh can be generated as electric energy. A winery that crushes 1000 tons of grape consume about 68 680 kWh, which are used for the winery operations (crushing, pressing, filtration, pumps use, cleaning of winery equipment and of installations) and refrigeration of wines and musts in fermentation. By the above, a winery can cover up to 45% of its energy requirements for the wine-making time utilizing the grape pomace that it generates itself. The performance of the power generating system using the biogas microturbine can be further increased using a cogeneration system, thus enabling to reach an 83% overall performance.

Fig. 6 – Dynamic response of the biogas microturbine. (a) Active power output. (b) Phase 'a' voltage and current.

REFERENCES

[1] Resumen cosecha 2010 por Delegación. Argentina: Instituto Nacional de Viticultura (I.N.V); 2010 [In Spanish].
[2] Celma AR, Rojas S, López-Rodríguez F. Waste-to-energy possibilities for industrial olive and grape by-products in Extremadura. Biomass and Bioenergy 2007;31(7):522–34.
[3] Meher Kotay S, Das D. Biohydrogen as a renewable energy resource—prospects and potentials. International Journal of Hydrogen Energy 2008;33(1):258–63.
[4] Keyser M, Witthuhn RC, Witthuhn L, Ronquest C, Britz TJ. Treatment of winery effluent with upflow anaerobic sludge blanket (UASB) – granular sludges enriched with *Enterobacter sakazakii*. Biotechnology Letters 2003;25(22):1893–8.
[5] Istrati L, Ciobanu D, Harja M, Ionaşcu D. Researches regarding inorganic accelerators using in pomace fermenting process. Journal of Agroalimentary Processes and Technologies 2007;13(2):241–8.
[6] Weiland P. Biogas production: current state and perspectives. Applied Microbiology and Biotechnology 2009;85(4):849–60.

[7] Ostrem K. Greening Waste anaerobic digestion for treating the organic fraction of municipal solid waste. Master Dessertation Thesis. Columbia University. 2008.

[8] Goldstein DJ. Air and steam Stripping of Toxic Pollutants, vol. I and II. U.S. Environmental Protection Agency Report; 1982. 683002.

[9] Khan I, Brimblecombe P, Clegg SL. Solubilities of pyruvic acid and the lower (C1-C6) carboxylic acids. Experimental determination of equilibrium vapour pressures above pure aqueous and salt solutions. Journal of Atmospheric Chemistry 1995;22(3):285—302.

[10] Snider JR, Dawson GA. Tropospheric light alcohols, carbonyls, and acetonitrile: concentrations in the southwestern United States and Henry's law data. Journal of Geophysical Research Atmosphere 1985;90(D2):3797—805.

[11] Márquez JL, Molina MG, Pacas JM. Dynamic modeling, simulation and control design of an advanced micro-hydro power plant for distributed generation applications. International Journal of Hydrogen Energy 2010;35(11): 5772—7.

[12] Grillo S, Massucco S, Morini A, Pitto A, Silvestro F. Microturbine control modeling to investigate the effects of distributed generation in electric energy networks. IEEE Systems Journal 2010;4(3):303—12.

[13] Guda SR, Wang C, Nehrir MH. Modeling of microturbine power generation systems. Electric Power Components and Systems 2006;34(9):1027—41.

[14] Deng Q. Chemical composition of dietary fiber and polyphenols of wine grape pomace skins and development of wine grape (cv. Merlot) pomace extract based films. Master Dessertation Thesis. Oregon State University. 2011.

[15] The MathWorks Inc.. SimPowerSystems for use with Simulink: User's Guide. Available from: www.mathworks.com; 2011.